11-21-2020

Pump Operating Effects on the Transient Fluid Flow.

H. Mansour
Mechanical Power Engineering Department, Faculty of Engineering, Mansoura Univversity, El Mansoura Egypt

Mohamed Saad ElDin
Mechanical Power Engineering Department, Faculty of Engineering, Mansoura University, El Mansoura Egypt

Emad El Negeery
Mechanical Power Engineering Department, Faculty of Engineering, Mansoura University, El Mansoura Egypt

Ahmed Draz
Mantrac Co., Egypt, eahmeddraz@gmail.com

Follow this and additional works at: https://mej.researchcommons.org/home

PUMP OPERATING EFFECTS ON THE TRANSIENT FLUID FLOW

دراسة تأثيرتشغيل المضخة على السريان الانتقلى للموائع

H. Mansour*, Mohamed S. Saad El Din*, Emad El Negeery*, and Ahmed Draz**

*Mechanical Power Engineering Department, Faculty of Engineering,Mansoura university, El Mansoura Egypt.
**Mantrac Co., Egypt

الملخص العربى

تحدث ظاهرة الطرق المائى فى خطوط الأنابيب نتيجة للتغير المفاجىء فى سرعة السائل يتبعها تغير مفاجىء فى الضغط ، وهى ظاهرة ذات آثار مدمره على أجهزه القياس المستخدمة وخطوط الأنابيب. يتناول البحث دراسه معملية ونظرية لتأثير التغير المفاجىء للتصرف فى حالة وجود مضخة فى خط الالانيب. تم تصميم دائرة هيدروليكية تحتوى على انبوبة فى نهايتها صمام يتم غلقه فجائياً واستخدمت وسائل القياس الازمة للحصول على توزيع الضغط عند مقاطع مختلفة على طول الأنبوبة. وكذلك تم تطوير نموذج رياضى ذو أربعه معادلات يتضمن الارتباط الديناميكى بين جسم الماسورة والمائع (معادلة الحركه لجسم الماسورة وعلاقة الانفعال لمادة جسم الماسورة) الى جانب منظومة المعادلتين والتى تحتوى معادلة الاستمراريه وكمية الحركة للمائع. وقد أمكن الحصول على نتائج تبين توزيع الضغوط عند مقاطع مختلفه للأنبوبة الى جانب توزيع الاجهاد على الأنبوبة وتوزيع سرعه السائل وكذلك الاستطاله الحادثه فى جسم الماسورة وذلك باستخدام طريقة المعادلات المميزة (MOC). وقد أظهرت للنتائج توافقا بين النتائج العملية و النظرية من حيث القيم العظمى للضغط والشكل وذلك فى ظروف حديه تحاكى ملظومة الأنابيب العملية. كذلك تم كتابة برنامج لحل هذه المعادلات باستخدام الحاسب الألى واختبرت مدى استجابة البرنامج لتأثير المتغيرات المختلفة. من نتائج البحث تم استنتاج اماكن القيم العظمى للضغط والاجهاد على طول الماسورة وذلك فى ازمنه غلق مختلفة للمحبس وتأثير وجود المضخة على ظاهرة الطرق المائى وهذه النتائج تفيد عند تصميم خطوط الأنابيب.

Abstract

A water hammer phenomenon due to sudden closure of a valve, with centrifugal pump at upstream, was studied both experimentally and numerically. Taking into consideration the fluid-structure interaction, it produced a four equations model (fluid continuity, fluid momentum, and pipe wall momentum and stress-strain equations). The four equations model was analytically solved using the method of characteristics to clarify, the centrifugal pump effect on the hammering waves. A FORTRAN program was developed to solve the model. The theoretical and experimental results indicated the pressure-time history at different positions along the pipe for different valve closing times. Also, predictions for stress-time history, fluid velocity-time history and structure velocity-time history were obtained at different positions along the pipe at different valve closing times. The obtained predictions are useful in pipeline design.

1-INTRODUCTION

Water hammer is the dynamic slam, bang, or shudder that occurs in pipes when a sudden change in fluid velocity creates a significant change in fluid pressure, that can destroy hydraulic devices and pipes. There are two models of equations used for analyzing water hammer problem with developing a numerical solution for solving these models. The first type is two equations model, and the second type is four equations model. *Two equations* model is a one-dimensional equation, and deals with parameters varied during transient occurred in fluid only and investigation of friction losses are estimated by applying a coefficient of pressure drop. Attributions of frictional losses are found in the valve and pipe, as consequence of fluid contractions and shear stress. *Four equations* model is two-dimension hyperbolic partial differential equation and describes the dynamic behavior of structure and fluid. The common aspect in these phenomena is the energy exchange between the fluid, and the structure; such exchange allows the writing of the continuity conditions necessary to drive the equations for the interactive system. This study indicates the effect of the centrifugal pump located at upstream end of the pipe line on the

hammering waves. **Thorley** (1969) developed the equations of motion for a cylindrical tube containing a fluid by considering the forces and moments effects on the tube wall. **Walker and Phillips** (1977) investigated a system of four linear, first-order, hyperbolic partial differential equations whose eigen-values give the wave velocities in the fluid and pipe wall. **Stuckenbruck et al.** (1985) calculated the magnitude of the acoustic wave speed influenced by properties of the fluid and the pipe materials based on a quasi-static control volume. **Wiggert et al.** (1985) studied the effect of elbow restraint on pressure transients. They showed that transient pressure in piped liquid is a function of structural restraint at elbows. The influence of structural damping on internal pressure during a transient pipe flow was studied by **Budny et al.** (1991). They used the four equations model of axial wave propagation with Poisson coupling, which includes viscous damping, to account for structural energy dissipation. **Sato et al.** (1991) stated that Zielke's technique of using the method of characteristics to simulate transient phenomena of a liquid pipeline is accurate and widely used. The interactions between axial wave propagation and transient cavitations in a closed pipe were studied by **Fan and Tijsseling** (1992). **Elansary and Contractor** (1994) studied how to reduce the undesirable dynamic pressure oscillation that occur in a simple pipeline due to valve closure and prevent the occurrence of column separation. **Kerb et al.** (1997) studied the transient fluid-structure interaction in a control valve, using numerical investigation on the interaction of a viscous incompressible fluid with a control valve by finite element method and new-mark approach. **Hawam** (2000) studied and analyzed numerically the water hammer phenomena, taken into consideration both pipe wall axial motion as well as outside

friction damping. **Bergant and Tijsseling** (2001) predicted the possible sources that may affect the wave form by using the classical water hammer theory including unsteady friction, cavitation, and a number of fluid-structure interaction effects. **Redaelli** (2002) introduced the equations that describe the dynamic behavior of a structure and a fluid and describe a formulation suitable for modeling the flow in domains with moving boundaries. **Tijsseling** (2003) investigated theoretically a method of exact calculation in terms of simple recursion. The method is valid for transient events only, because the calculation time grows exponentially with the duration of the event. **Kratz et al.** (2003) derived two methods which are used in fluid-structure analysis; (*i*) uncoupled method, where a fluid-dynamic analysis is carried out with the assumption of a fixed structure; next with resultant time dependent pressure and reaction forces the structural analysis is made. This method neglected the effect of fluid-structure interaction. (*ii*) coupling method that coupled of both parts, simultaneously calculated the fluid and structure response under consideration of fluid-structure interaction. They recommended that fluid-structure interaction should be taken into account. Static and dynamic analyses of a piping system at NASA were done by **Nieves** (2004); he determined the natural frequencies, static stress and the limitations of the pipeline system. Also he developed simple chart characterizing the relation between stress and location along the length of the pipe line for all segments. Tijsseling (2007) studied a one-dimensional mathematical model which described the acoustic behavior of thick-walled liquid-filled pipes. The model uses was based on conventional water-hammer and beam theories, taking into account fluid–structure interaction. He stated that the resulting fluid–structure interaction four-equation model

has small correction terms and factors accounting for the wall thickness. Also Exact solutions of this model showed that these corrections were important only for very thick pipes, with, say, a radius/thickness ratio smaller than 2. Tijsseling (2009) found exact solutions to the problem of two coupled axially-vibrating liquid-filled pipes. Fluid-structure interaction at pipe ends and junction, and along the pipe because of axial-radial Poisson contraction, is taken into account. The solutions obtained for a water hammer problem showed unprecedented details that resemble noise. **Ismaier** and **Schlücker** (2009) investigated experimentally the dynamic interaction between water hammer and pressure pulsations. Different measurements at this testing facility showed that pulsating centrifugal pumps can damp pressure surges generated by fast valve closing. They also showed that 1-dimensional fluid codes can be used to calculate this phenomenon. Furthermore they presented that pressure surges pass centrifugal pumps almost unhindered, because they are hydraulic open. **Djebedjian. et.al.** (2009) linked between water hammer in the distribution systems and optimization in designing and planning networks, taking into consideration water hammer event. The main objective of this study is to investigate numerically and experimentally the effect of the pump on the hammering wave generated in a pipeline due to sudden valve closure. The effect includes the maximum and minimum pressures, maximum stress, maximum structural velocity, and maximum flow velocity and damping time for each wave, according to different valve closing times. The mathematical model for hammering wave was driven using the method of characteristics. The mathematical model is four equations model. A comparison between theoretical study and the experiments is presented.

2-EXPERIMENTAL SET-UP

2-1 Experimental Test-Rig:
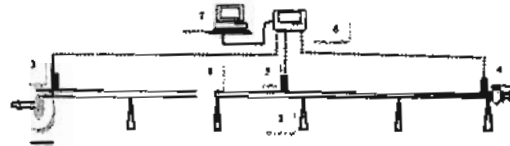
1- Centrifugal pump 2- Support 3- Check valve 4- Ball valve 5- Sensor 6- Data logger 7- Computer 8- Joint
Figure 1 Experimental test-rig

Figure 1 show a schematic diagram of the test-rig which was used to observe the dynamic behavior of pressure resulting from a sudden valve closure during pump operation. The test-rig is basically consists of five main parts;

2-1-1 Water Supply

It consists of a centrifugal pump with characteristic curve
$P = -5410*Q + 4.181$ where P is the pressure (*bar*), and Q is the discharge, (m^3/s).

2-1-2 Test Section

The test section is a straight pipe manufactured from white cast iron, with 14.35m length, 25.4mm inner diameter and 34mm outer diameter. The pipe material has the following properties: pipe density of 7250 kg/m^3, tensile stress of 290 GN/m^2, Poisson ratio of 0.23, and modulus of elasticity of 120 GN/m^2. The pipe is placed in a horizontal plane and mounted to the ground to prevent the axial motion with clamps of pitch 2.7m

2-1-3 Hammering Generation Device

The water hammer was produced by a rapid valve closure; the valve is suddenly closed by means of a spring attached to the handle of the valve. Closing time can be changed by shortening or extending the spring which is attached to the valve.

2-1-4 Measuring Devices

The dynamic pressure is sensed by the pressure transducer and the signal is to be

sent to the data logger which is the media between sensors and computer where the measured values are restored in a data file. The pressure is sensed by the pressure transducers located at three sections; at the pump outlet, $x_{r1}=0.0027$, just before the valve, $x_{r3}=0.998$ and at $x_{r2}=0.56$ where (x_{ri} is dimensionless distance and defined as (distance/ pipe length), L = 14.35).

Pressure transducer

The used pressure transducer has a pressure range of 0:8 *bar*, power source input of 12 *Volt DC* and transducer output is in Ampere according to pressure value which is converted to variation in *volt*. The uncertainty of the pressure transducer as estimated by the manufacturer is ± *3* percent of maximum pressure range. The pressure transducer was calibrated using the circuit shown in Fig. (2) and the following equation was obtained;

$$P= (V -11.61607143)/ 0.4732142857 \quad (1)$$

where V is in volt and P is the pressure in bar.
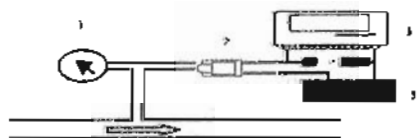
1- Borden tube pressure gauge (0:25 bar)   2- Pressure transducer
3- Avometer   4- Resistance 1000Ω   5- 12 Volt battery

Figure 2 Pressure transducer calibration circuit

Pressure gauge

The pressure gauge used is a Bourdon tube gauge has a range 0:25 *bar* and its accuracy is ± 2 % of full scale. The gauge have indicator to indicate the maximum pressure values.

2-1-5 Recording Devices

The data logger with type (VELLEMAN_Kit, (K8047)) is used as media between pressure transducer and computer. The data logger has four coupled input channels, with a maximum input Volt equal to 30 *Volt DC*, the least count is 10 *mV* and 100 samples per second. The major source of the experimental uncertainty is the data logger, which takes 100 samples per second, where as theoretically the pressure varies 1000 times during one second

2-2 Experimental Procedure

The experimental procedure is as follows;
- Assure that the test-rig is rigidly clamped horizontally to the ground.
- Open the ball valve to fully opened position, then the pump is started to pump water through the pipe until all air is removed completely from the pipe and steady-state flow is attained.
- Check the pipeline and all joints against any water leakage.
- Switch on computer and assure that data logger is powered.
- Check data logger by reference values as 1.5 Volt battery.
- Check all electrical lines and joints against cut-off and open circuit.
- The valve is suddenly closed under the effect of the spring, and the closing time is measured by oscilloscope (BK PRECISION (2190B), dual time base, 5mV/division sensitivity, sweeps 5ns/division, 30 V maximum and 100MHz sample).
- The pressure is measured at three positions, just at pump exit, just before the valve and at the middle of the pipe.
- Open the valve completely again and wait until steady-state condition is attained.
- Change the spring stiffness many times to change the closing time and repeat the previous steps.

All the data are recorded as voltage values, and after that they transformed to pressure values using Eq. (1).

3- MATHEMATICAL FORMULATION

The four-equation model is considered in this study. Assuming that:

- The fluid remains in liquid phase at all the time, no cavitation occurs.
- Velocity of fluid in the direction of the axis of the pipe is uniform over any cross-section of pipe (one-dimensional flow).
- The pressure is uniform over a transverse cross-section of the pipe and is equal to the pressure at the center line of the pipe.
- Pipe material remains in elastic zone.
- Fluid shear is expressed in terms of constant friction coefficient (unsteady shear stress are neglected).
- For all relations, the radial strain of the tube wall is negligible compared to radius of curvature of the middle surface.
- All points on radial plane before deformation occurs remain plane after deformation.
- The bulk modulus for the liquid is constant.

inviscid slightly compressible liquid and fluid velocity is much smaller than the speed of sound in the pipe, hence the fluid motion is governed by a three equations system given by Walker and Phillips (1977) in the form:

$$\frac{1}{K}\frac{\partial P}{\partial t} + \frac{\partial V_r}{\partial r} + \frac{V_r}{r} + \frac{\partial V_x}{\partial x} = 0 \tag{2}$$

$$\frac{\partial P}{\partial x} + \rho_f \frac{\partial V_x}{\partial t} = 0 \tag{3}$$

$$\frac{\partial P}{\partial r} + \rho_f \frac{\partial V_r}{\partial t} = 0 \tag{4}$$

In addition, the pipe motion is governed by the equations for small deformation, elastic; stress problem. Budny et al. (1991) give that;

$$\frac{\partial \sigma_x}{\partial x} - \rho_p \frac{\partial U_x}{\partial t} = 0 \tag{5}$$

$$\rho_p e \frac{D}{2}\frac{\partial U_r}{\partial t} - \frac{DP_o}{2} + e\sigma_\theta = 0 \tag{6}$$

$$\frac{\partial \sigma_x}{\partial t} - \frac{E}{\left(1-\nu^2\right)}\left(\frac{\partial U_x}{\partial x} + \frac{\nu \dot{U}_r}{2D}\right) = 0 \tag{7}$$

$$\sigma_\theta - \frac{E}{\left(1-\nu^2\right)}\left(\frac{2\dot{U}_r}{D} + \nu\frac{\partial \dot{U}_x}{\partial x}\right) = 0 \tag{8}$$

Budny et al. (1991) used the four equations model considering the axial pipe motion and implementing distributed damping outside the pipe wall as well as inside shear stress. The four equations are rewritten here in slightly modified form in terms of fluid variables: the pressure P and the fluid flow velocity V, as well as pipe variables: the axial pipe stress σ and the pipe axial displacement velocity U, as follows:

Fluid continuity

$$\frac{\partial P}{\partial t} - 2\nu K \cdot \frac{\partial U}{\partial x} + K \cdot \frac{\partial V}{\partial x} = 0 \tag{9}$$

Fluid momentum

$$\frac{\partial P}{\partial x} + \rho_f \frac{\partial V}{\partial t} + \tau_o \pi \frac{D}{A_f} = 0 \tag{10}$$

Pipe momentum

$$\frac{\partial \sigma}{\partial x} - \rho_p \frac{\partial U}{\partial t} + \tau_o \pi \frac{D}{A_p} - C_x \frac{U}{A_p} = 0 \tag{11}$$

Stress-strain

$$\frac{\partial \sigma}{\partial t} - E \frac{\partial U}{\partial x} - \frac{\nu D}{2e}\frac{\partial P}{\partial t} = 0 \tag{12}$$

The modified bulk modulus K^* of elasticity is taken into consideration in the fluid-pipe interactions.

The four partial differential equations (fluid continuity, fluid momentum, pipe momentum, and stress-strain equations) are transformed into ordinary differential equations by the method of characteristics. First the relation for total time derivative of any quantity (which may be P, V, σ, and U) for an observer traveling along the pipe at wave speed λ is taken as:

$$\frac{\partial(\theta)}{\partial t} + \lambda \frac{\partial(\theta)}{\partial x} = \frac{d(\theta)}{dt} \tag{13}$$

Then Equations (9) to (12) are transformed into four ordinary differential equations.

The relation for the eigen-values (wave speeds) is:

$$\lambda_i^2 = \frac{1}{2}\left(a_f^2 + a_p^2 + 2\nu^2 a_f^2 \frac{d}{b} \right)$$

$$\pm \frac{1}{2}\sqrt{\left(a_f^2 + a_p^2 + 2\nu^2 a_f^2 \frac{d}{b} \right)^2 - 4a_f^2 a_p^2} \tag{14}$$

where

$$a_f^2 = \frac{K^*}{\rho_f}, \quad a_p^2 = \frac{E}{\rho_p}, \quad b = \frac{P_p}{\rho_f}, \quad d = \frac{D}{2e}$$

and

$i=1$, or 2 λ represents the positive or negative axial pipe wave speed

$i=3$, or 4 λ represents the positive or negative liquid wave speed.

As noted by Stuckenbruck et al. (1985), if the second order Poisson term is dropped from the above equation, the classical fluid wave speed prediction for a pipe anchored throughout against axial motion is obtained. The four compatibility equations, for $i = 1, 2, 3,$ and 4 have the form;

$$-\frac{2\nu\lambda_i}{\rho_p\left(\lambda_i^2 - a_p^2\right)}\frac{d\sigma}{dt} - \frac{2\nu\lambda_i^2}{\left(\lambda_i^2 - a_p^2\right)}\frac{dU}{dt} + \left(\frac{\lambda_i}{K^*} - \frac{2\nu^2 d\lambda_i}{\rho_p\left(\lambda_i^2 - a_p^2\right)} \right)\frac{dP}{dt}$$

$$+ \frac{dV}{dt} + \frac{2\nu\lambda_i^2}{b\left(\lambda_i^2 - a_p^2\right)}\left(\frac{\tau_o \pi D}{\rho_f A_p} - \frac{C_x \dot{U}}{\rho_f A_p} \right) + \frac{\tau_o \pi D}{\rho_f A_f} = 0 \tag{15}$$

Each compatibility equation is integrated along its appropriate characteristic line, and algebraic equations are produced which are solved on a time-space grid. The algebraic equations are solved for the dependent variables (P, V, σ and U) by using the method of characteristics.

3-1 Boundary Conditions

At either end of a single pipe, only one of the compatibility equations is available in four variables. For each of the upstream and downstream ends, there are three points which are taken as boundary points.

3-1-1 Upstream Boundary Conditions

1- Boundary condition at point ($N=1$)
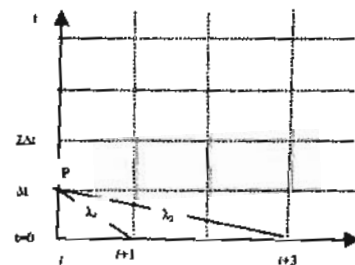
Figure (3-a) x-t grid for solving single-pipe problem at point ($N=1$)

At $N=1$ the centrifugal pump with known head-discharge curve is described by Equation (16). The pump is supplying flow from a constant pressure suction source which equals to the atmospheric pressure.

$$P_{(1,j)} = P_s + \rho g A V_{(1,j)}\left(a_1 + a_2 A V_{(1,j)} \right)$$

$$P_{(i-1,j)} = P_{(i-3,j)} = 0 \tag{16}$$

$$\sigma_{(i-1,j)} = \sigma_{(i-3,j)} = 0$$

$$U_{(i-1,j)} = U_{(i-3,j)} = 0$$

$$V_{(i-1,j)} = V_{(i-3,j)} = 0$$

By substituting the previous values of Equation (16) in Equation (15) to obtain the values of V, U, and σ at point ($N=1$) at any time t and taking into consideration that $P_{(1,j)}=P_{(i,j)}$ in the previous equations.
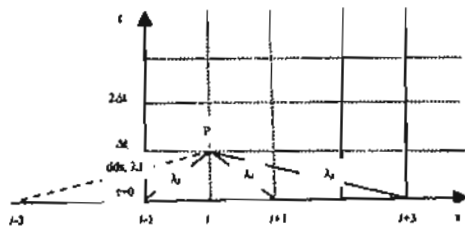
## 2- Boundary condition at point ($N=2$)

Figure (3-b) x-t grid for solving single-pipe problem at point ($N=2$)

At point $N=2$, to obtain the values of P, V, U, and σ at point $N=2$, and at time t the following equations are solved simultaneously by using the Newton-Raphson method and taking into consideration the following values:

$$P_{(i-3,j)} = P_{dds}(1) = P_{sh}$$

$$V_{(i-3,j)} = V_{dds}(1) = [2*V_s(1) +V(1)]/3$$

$$U_{(i-3,j)} = U_{ddds}(1) = [2*U_{ds}(1) +U_d(1)]/3$$

$$\sigma_{(i-3,j)} = \sigma_{dds}(1) = [2*\sigma_s(1) +\sigma(1)]/3$$

$$(17)$$

By substituting the previous values in Equation (17) in Equation (15) to obtain the values of P, V, U, and σ at point ($N=2$) at any time t.

3- Boundary condition at point ($N=3$)
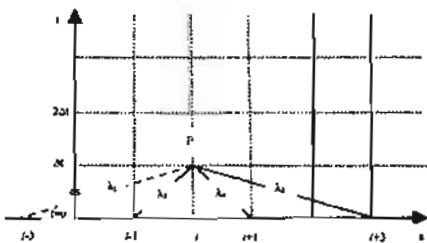
Figure (3-c) x-t grid for solving single-pipe problem at point ($N=3$)

At point $N=3$, to obtain the values of P, V, U, and σ at point $N=3$, and at time t the following equations are solved

simultaneously by using the Newton-Raphson method, and the values:

$$P_{(i-3,j)} = P_{ds}(1) = P_{sh}$$

$$V_{(i-3,j)} = V_{ds}(1) = [V_s(1) + 2*V(1)]/3$$

$$U_{(i-3,j)} = U_{dds}(1) = [U_{ds}(1) +2*U_d(1)]/3 \qquad (18)$$

$$\sigma_{(i-3,j)} = \sigma_{ds}(1) = [\sigma_s(1) + 2*\sigma(1)]/3$$

By substituting the previous values in Equation (18) in Equation (15) to obtain the values of P, V, U, and σ at point ($N=3$) at any time t.

3-1-2 Downstream boundary conditions

At the downstream end ($x=L$), a valve is discharging fluid into the atmosphere. Hence, the pressure drop across the valve is equal to the gauge pressure just before the valve. The coefficient of pressure drop for a wide open valve h_v is defined as:

For　　　　　$x=L$　,$t<0$

$$P_{Ns} = h_v \rho_f \frac{V^2}{2} \qquad (19)$$

The valve is closed during the time t_c. During valve closure, the valve hydraulic resistance increases with time until reaching infinity when it is fully closed. By assuming that the valve is closed in no time, the source of non-linearity is eliminated and helps understanding many aspects of fluid-pipe coupling mechanism, which is the main objective of this study. This simplification yields the upper bounds for maximum pressure and stress which are important for pipe design, compared to cases where $t_c > 0$. As valve closure optimization is an important subject, hence, the hydrodynamic boundary condition for positive time is simplified to:

For:　$x=L$　,　$t \geq 0$

$$V = 0 \qquad (20)$$

1- Boundary condition at point (N$_s$)
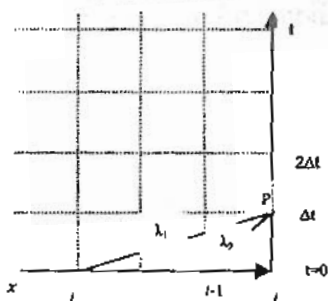
Figure (4-a) x-t grid for solving single-pipe problem at point (N$_s$)

At point N$_s$, to obtain the values of P, U, σ at any point N$_s$, and at time t the following equations are solved simultaneously by using the Newton-Raphson method and solving Equation (15) after substituting the following values,

$$P_{(i+1,j)} = P_{(i+3,j)} = 0$$

$$V_{(i+1,j)} = V_{(i+3,j)} = 0$$

$$U_{(i+1,j)} = U_{(i+3,j)} = 0 \tag{21}$$

$$\sigma_{(i+1,j)} = \sigma_{(i+3,j)} = 0$$

2- Boundary condition at point (N$_s$-1)
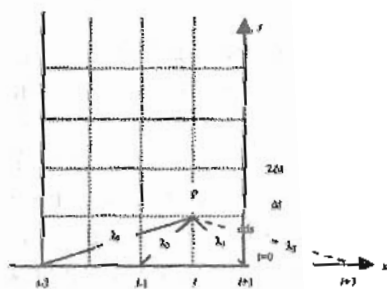
Figure (4-b) x-t grid for solving single-pipe problem at point (N$_s$-1)

At point N$_s$-1, to obtain the values of P, V, U, and σ at any point N$_s$-1, and time t the following equations are solved simultaneously by using the Newton-Raphson method and solving Equation (15) after substituting the following values:

$$P_{(i+3,j)} = P_{dds}(N_s) = [2*P_s(N_s) + P(N_s)]/3$$

$$V_{(i+3,j)} = V_{dds}(N_s) = [2*V_s(N_s) + V(N_s)]/3 \tag{22}$$

$$U_{(i+3,j)} = U_{dds}(N_s) = [2*U_{ds}(N_s) + U_d(N_s)]/3$$

$$\sigma_{(i+3,j)} = \sigma_{dds}(N_s) = [2*\sigma_s(N_s) + \sigma(N_s)]/3$$

3- Boundary condition at point (N$_s$-2)
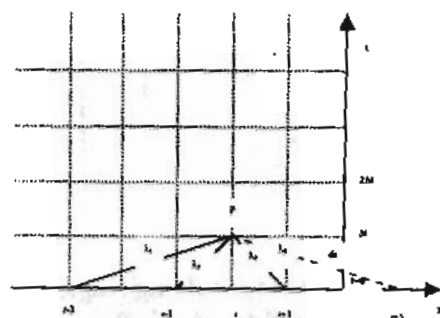
Figure (4-c) x-t grid for solving single-pipe problemat point (N$_s$-2)

At point N$_s$-2, to obtain the values of P, V, U, and σ at any point N$_s$-2, and time t the following equations are solved simultaneously by using the Newton-Raphson method and solving Equation (15) after substituting the following values:

$$P_{(i+3,j)} = P_{ds}(N_s) = [P_s(N_s) + 2*P(N_s)]/3$$

$$V_{(i+3,j)} = V_{ds}(N_s) = [V_s(N_s) + 2*V(N_s)]/3 \tag{23}$$

$$U_{(i+5,j)} = U_{dds}(N_s) = [U_{ds}(N_s) + 2*U_d(N_s)]/3$$

$$\sigma_{(i+3,j)} = \sigma_{ds}(N_s) = [\sigma_s(N_s) + 2*\sigma(N_s)]/3$$

3-2 Initial Conditions

Initial conditions are the steady-state conditions at the moment when the valve is widely open and steady operation of pump. First, the pressure (P) is linearly decreasing along the pipe length as follows:

$$P_{(i,0)} = P_p - \frac{f_x}{D}\frac{V^2}{2g} \tag{24}$$

at steady-state and assuming that:

$$V_{(i,0)} = constant = V_{main} \tag{25}$$

Due to this pressure distribution the stresses and pipe wall velocity is solved by neglecting the radial stress as follows:

$$\sigma_{(i,0)} = P_{(i,0)} \frac{(r_o^2) + (r_i^2)}{(r_o^2) - (r_i^2)} \tag{26}$$

Knowing the pump discharge Q_{p1}, $Pp1$ is obtained from the performance curve of pump.

$$\dot{U}_{(i,0)} = \frac{a_p}{E}\sigma_{(i,0)} \tag{27}$$

4- RESULTS AND DISCUSSION

The results demonstrate the effect of centrifugal pump at upstream end of the pipe during the transient condition. In this section, a comparison between the numerical and the experimental results is presented.

4-1 Experimental Results

Typical results for the conditions of rigidly fixed clamps with an initial steady-state Reynolds number of $3.67*10^4$, and at positions $x_{r1}=0.0027$, $x_{r2}=0.56$, and $x_{r3}=0.998$ are displayed. Figures (5), and (7), (9) illustrate the pressure-time history for this case of study (fixed clamps), where (pressure ratio, P_r = actual pressure / initial pressure). From these figures it can be noted that for the same initial boundary conditions, the pressure-time history curves at the different positions along the pipeline have the same trend as that obtained numerically by the four equations model Figures (6, 8, 10) but Figures (9- b, c) and Figures (10- b, c) have a trend difference. The pressure-time history curves have some variations in the maximum pressure value and differences in the frequency and damping time. This difference is due to the data logger responsibility.

4-2 NUMERICAL RESULTS

Theoretical results are calculated at different closing times from $t_c=t_{wp}$ to $t_c=40t_{wp}$; the sample of results are taken at closing times $t_c= t_{wp}$, $20twp$, and $40t_{wp}$.

4-2-1 Program Validation

The validity of the FORTRAN program (WHPUMP2) developed by Streeter (1993) and is checked by solving an example, [17], to assure program accuracy. The results obtained are close enough with that obtained in [17]. The previous program is taken and developed to solve the four equations model, (WHPUMP4), to predict the pressure, fluid velocity, stress, and strain versus time variation. The program is fed with properties of fluid, pipe, and pipe fixation, valve closing time and pump characteristics curve.

4-2-2 Pressure-Time Variations Analysis

Figures (6), (8), and (10) illustrate the pressure-time variation using the four equations model at different closing time values, $(t_c= t_{wp}, 20t_{wp}, 40t_{wp})$ and at different positions along the pipe, where the pressure transducers are located. From these figures, it can be seen that; the pressure wave peaks (and intermediate pressure wave peaks) take more rectangular shape at downstream locations. Also, the maximum pressure value increases at downstream locations, and reaches its maximum value at locations near the valve with closing time less than or equals $20t_{wp}$, but when the closing time is greater than $20t_{wp}$, the maximum pressure decreases at downstream locations from the pump.
An intermediate pressure wave peaks resulted from impeller effect appears at points near the pump. Also, the damping time increases at downstream locations from the pump.
At different closing times and different distances from the pump, the maximum

pressure value decreases with increasing the closing time, and the damping time decreases with increasing the closing time.

4-2-3 Stress-Time Variation Analysis

Figures (11) to (13) illustrate the stress-time variation at different closing times, ($t_c = t_{wp}$, 20 t_{wp}, 40 t_{wp}) and different positions along the pipe.

At the same closing time, and $t_c < 10 \ t_{wp}$ and different positions from the pump, at the downstream location along the pipeline the maximum stress value increases. Also the positive stress waves are higher than the negative stress waves at the same position along the pipeline, and the damping time for stress waves is semi equals the damping time for pressure waves at the same condition.

At the same closing time, and $t_c \geq 10 \ t_{wp}$ and different distances from the pump, the maximum stress occurs at the intermediate positions along the pipe line, and the negative stress waves are stronger than the positive stress waves at the same section along the pipeline. Also, the damping time for stress waves is semi equals the damping time for pressure waves which have the same conditions.

At different closing times, and $t_c \leq 10 \ t_{wp}$ and different distances from the pump, the maximum stress occurs near the valve, while the minimum stress occurs near the pump.

At different closing times, and $t_c \geq 10 \ t_{wp}$ and different distances from the pump, the maximum stress occurs at the intermediate positions, and the minimum stress occurs at both positions near the pump and near the valve, and as the closing time increases the stress reaches its maximum values at the moment the valve is fully closed.

At different closing times, and $t_c \leq 40 \ t_{wp}$ and different distances from the pump, as the closing time increases the maximum stress values (positive and negative) decreases. Also, the wave peaks become smooth as the closing time increases. And

the stress waves damping time increases as the closing time increases, and the damping time for pressure wave is less than damping time for stress wave at the same conditions.

4-2-4 Fluid Velocity–Time Variation Analysis

Figures (14) to (16) illustrate the fluid velocity-time variation at different closing times ($t_c = t_{wp}$, 20 t_{wp}, 40 t_{wp}) and different positions along the pipe.

At the same closing time and different distances from the pump, the maximum value of fluid-velocity occurs at the intermediate positions of the pipe line, and decreases on both ends of the pipeline. Also, the wave peaks take more regular shape at approached locations from the pump.

At different closing times and different distances from the pump, as the closing time increases, the damping time increases. Also, the absolute negative fluid velocity decreases as closing time increases; this may be attributed to the impeller effect.

4-2-5 Structure Velocity-Time Variation Analysis

Figures (17) to (19) describe the structure velocity-time variation at different closing times, ($t_c = t_{wp}$, 20t_{wp}, 40t_{wp}) and different positions along the pipe.

At closing time $t_c < 20 \ t_{wp}$, the maximum structure velocity occurs at intermediate positions, whereas at closing time $t_c \geq 20 \ t_{wp}$ the maximum structure velocity occurs at positions near the pump, and the damping time is equal to the damping time for the stress waves.

At different closing times and different distances from the pump, as the closing time increases the maximum structure velocity decreases. Also, as the closing time increase the damping time for structure velocity wave's increase.

4-3 Comparison between Numerical and Experimental Results

The comparison between numerical results, Figures (6, 8, 10), and experimental results, Figures (5, 7, 9), shows good agreement for the values of maximum and minimum pressures. The difference between experimental and numerical results is due to the accuracy of the devices used in the measurements, e.g. as the data logger takes 100 samples per second and the real variations are 1000 variations per second. Also, the damping time obtained from the numerical results is lower than that from the experiments. This can be attributed to the accuracy of the measuring devices.

5- CONCLUSIONS

The present study investigated numerically and experimentally the effect of the pump on the hammering wave generated in a pipeline due to sudden valve closure. The following conclusions were obtained:

- A series of pressure-time history curves were obtained numerically and experimentally in case of using pump at the upstream end. The trend of numerical curves agrees enough with that obtained experimentally.
- Numerical and experimental results indicated that the pressure reaches the maximum value near the valve and decreases as the downstream location along the pipeline decreases.
- A series of stress-time history curves were obtained numerically. The curves indicated that the maximum stress values occur at the middle positions of the pipeline and decreases along the two sides of the middle position.
- Effect of valve closing time was numerically explored, the results indicated that as the valve closing time increases the maximum pressure value decreases.
- Stress waves energy and pressure wave's energy represent the total energy of the hammering waves. Stress values effect on the pipe during transient flow is calculated only by using the four equations model. Stress waves travel along the pipe with speed approximately four times more than the pressure wave.
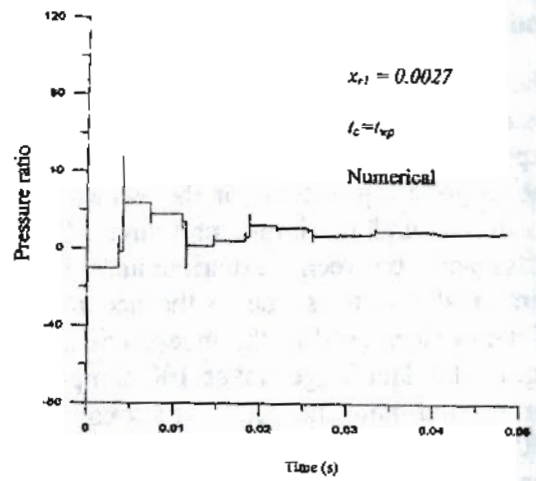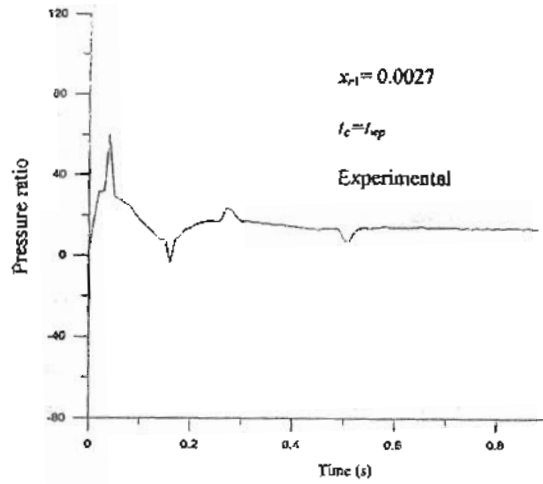
Figure (5-a)

Figure (6-a)
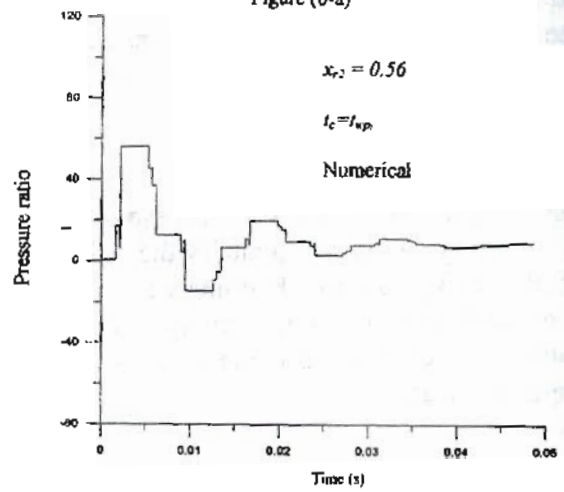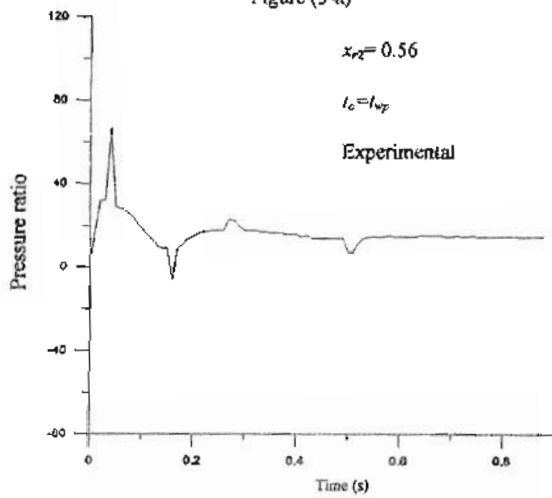
Figure (5-b)

Figure (6-b)
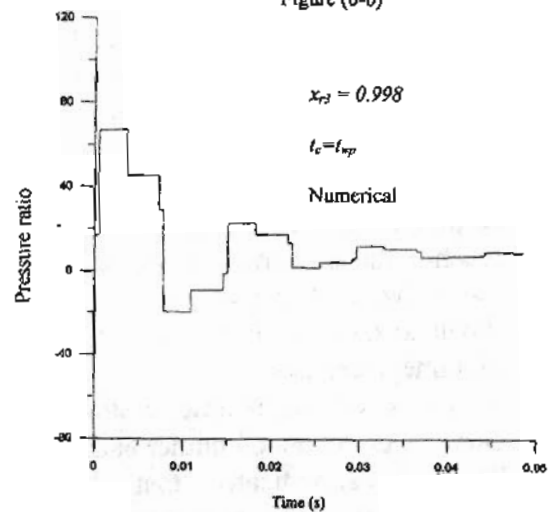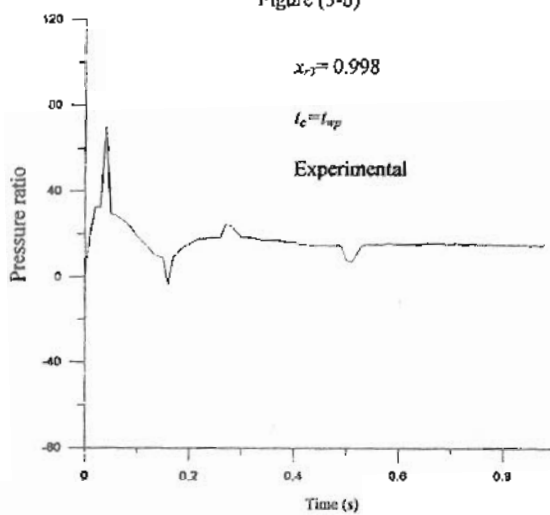
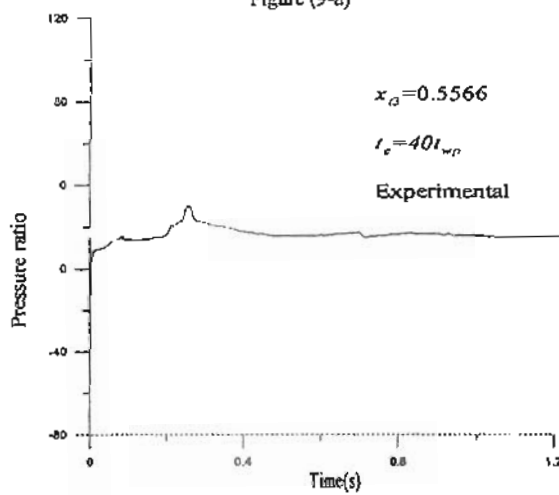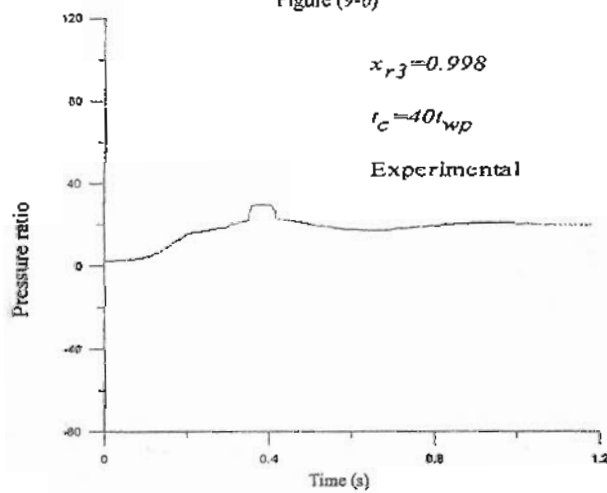
Figure (5-c)

Figure (6-c)

Figure (5) Experimental pressure-time history at three positions along the pipe at $t_c = t_{wp}$, and $P_i = 0.3bar$
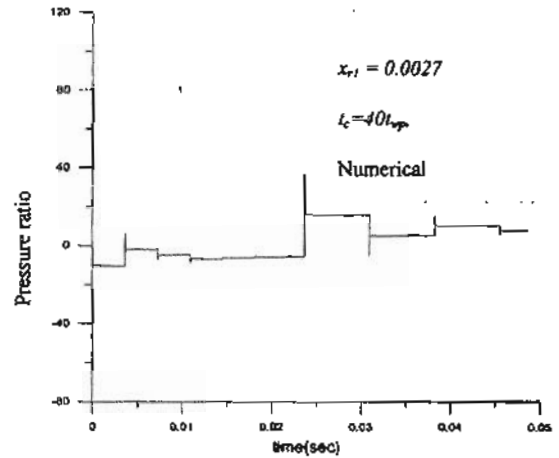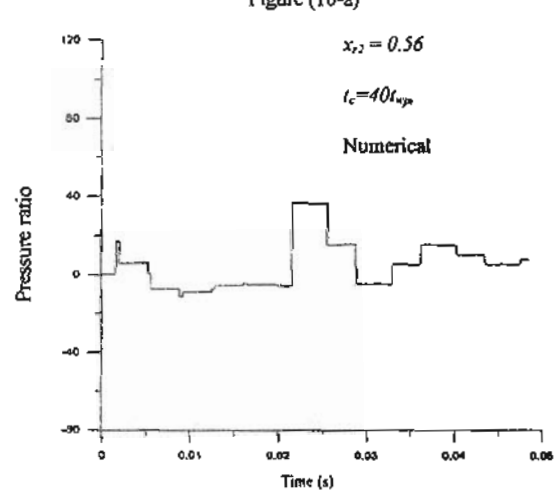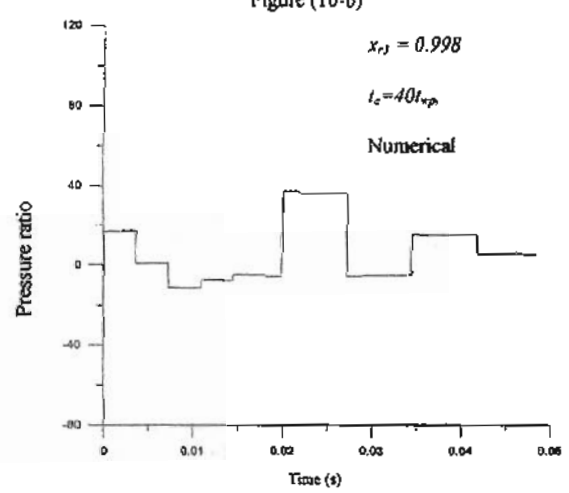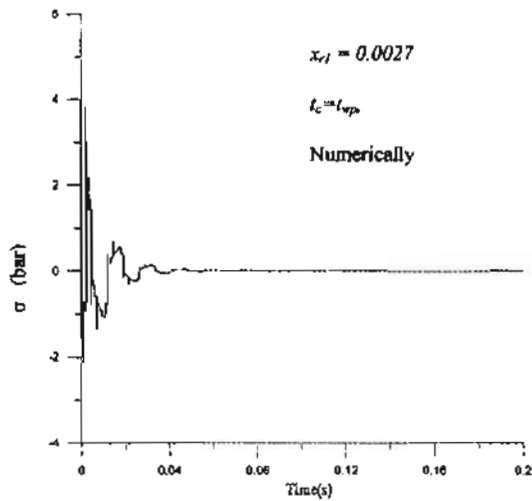
Figure (6) Predicted pressure-time history at three positions along the pipe at $t_c = t_{wp}$, and $P_i = 0.3bar$
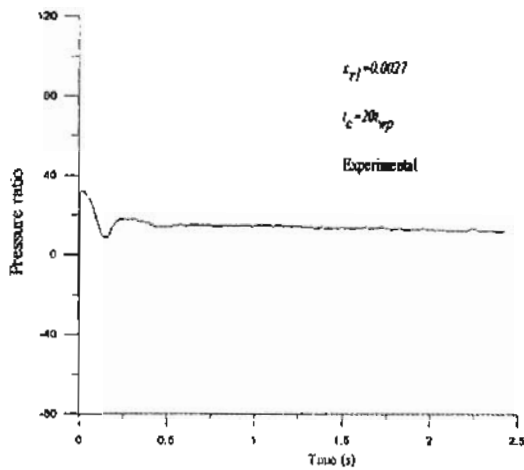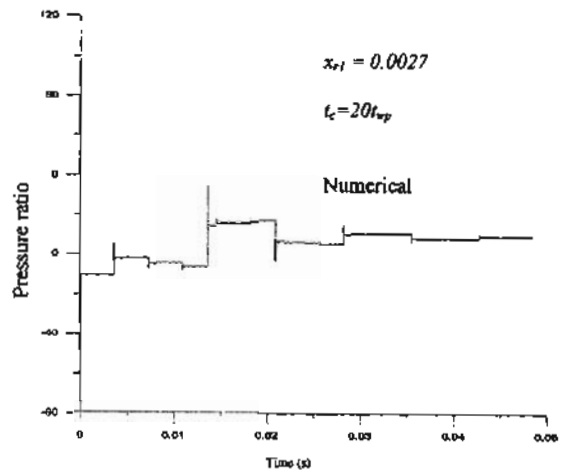
Figure (7-a)

Figure (8-a)
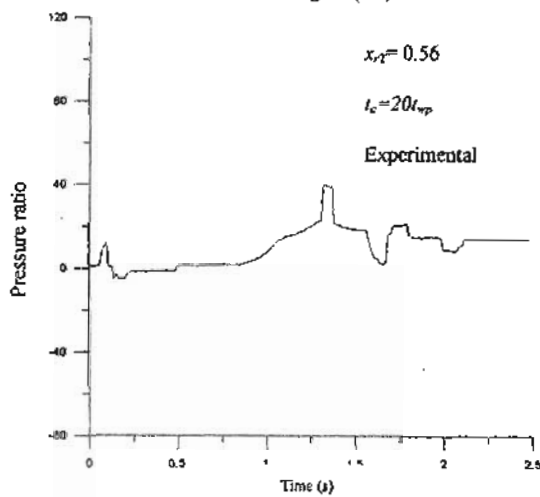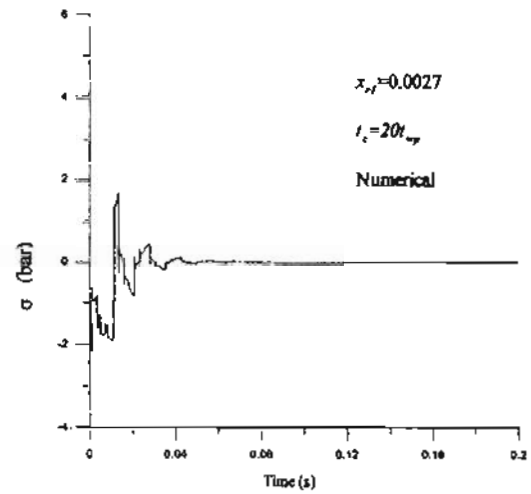

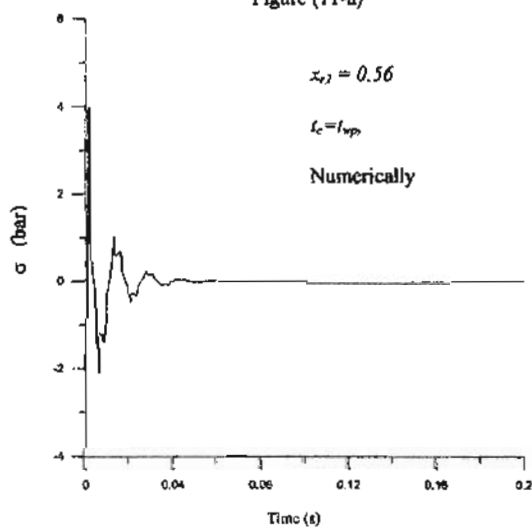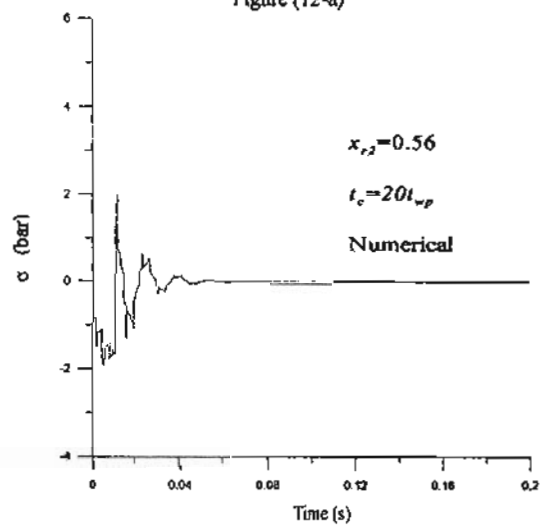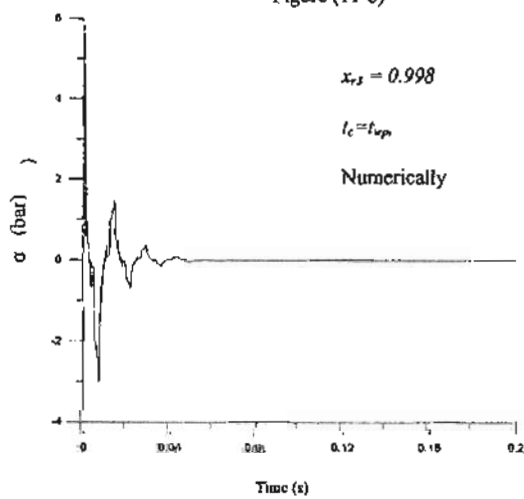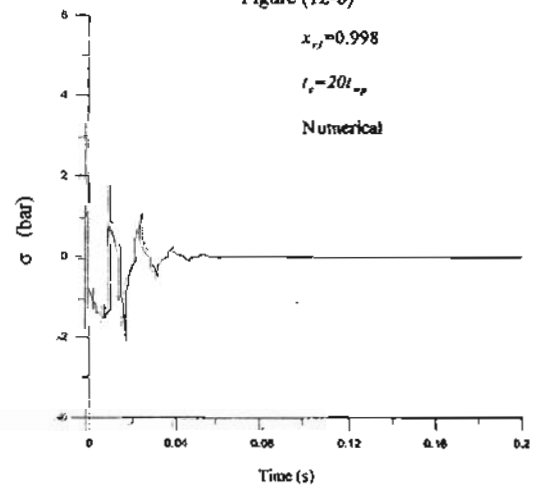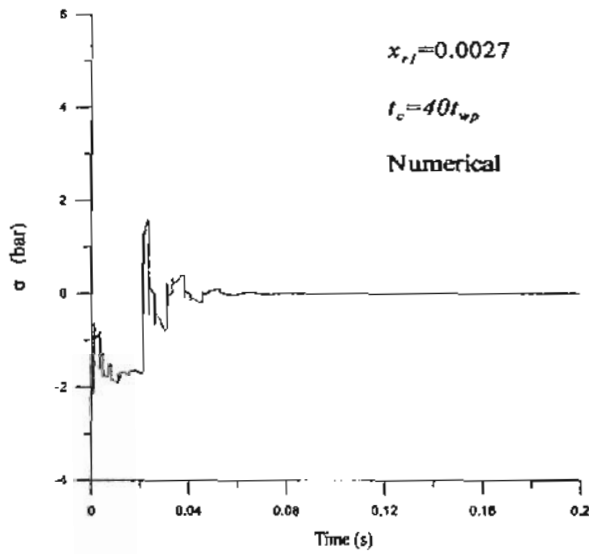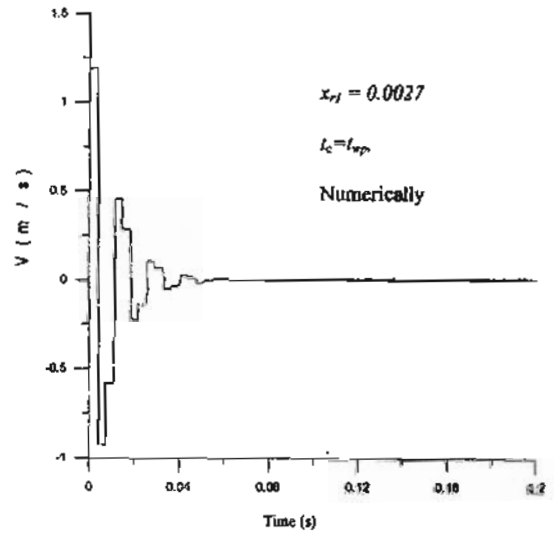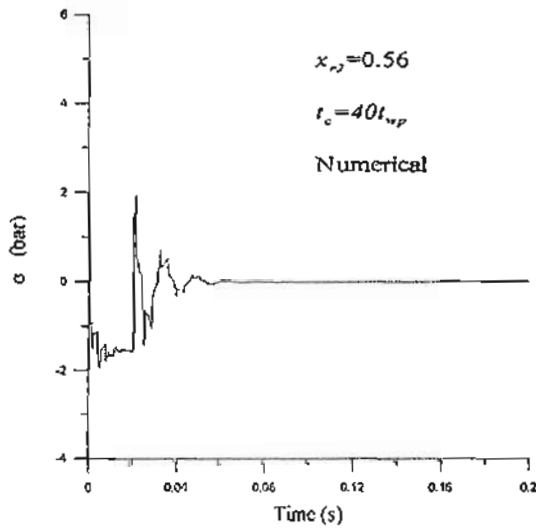Figure (7-b)
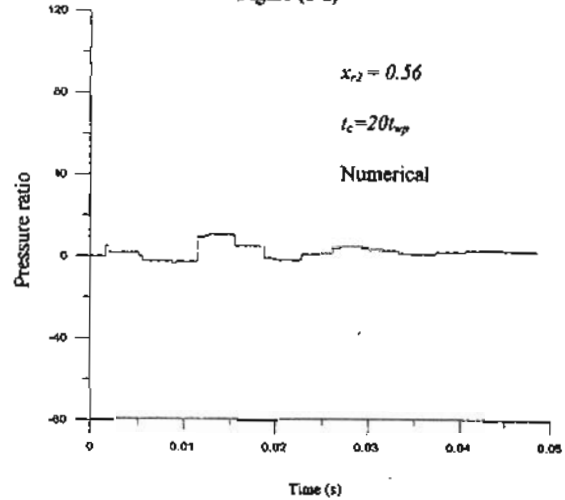
Figure (8-b)
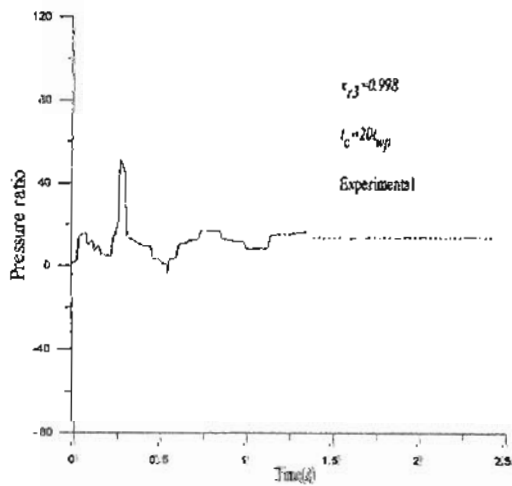
Figure (7-c)
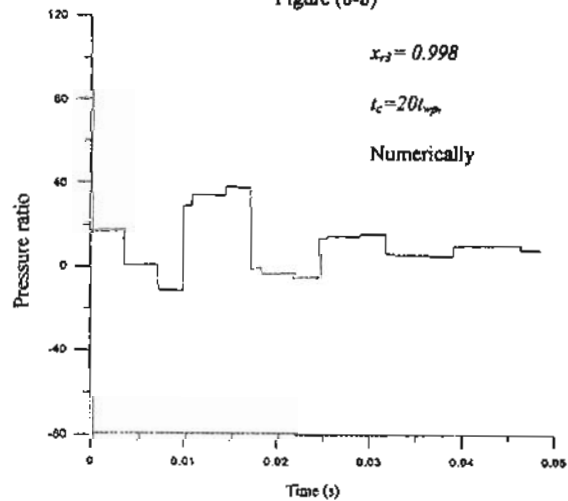
Figure (8-c)

Figure (7) Experimental pressure-time history at three positions along the pipe at $t_c=20t_{wp}$ and $P_i=0.3bar$

Figure (8) Predicted pressure-time history at three positions along the pipe at $t_c=20t_{wp}$ and $P_i=0.3bar$

$x_{r1} = 0.0027$

$t_c = 40t_{wp}$

Experimental

Figure (9-a)

$x_{r1} = 0.0027$

$t_c = 40t_{wp}$

Numerical

Figure (10-a)

$x_{r2} = 0.5566$

$t_c = 40t_{wp}$

Experimental

Figure (9-b)

$x_{r2} = 0.56$

$t_c = 40t_{wp}$

Numerical

Figure (10-b)

$x_{r3} = 0.998$

$t_c = 40t_{wp}$

Experimental

Figure (9-c)

$x_{r3} = 0.998$

$t_c = 40t_{wp}$

Numerical
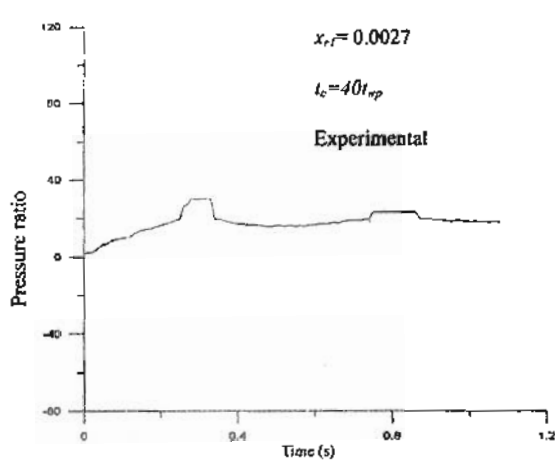
Figure (10-c)

Figure (9) Experimental pressure-time history at three positions along the pipe at $t_c = 40t_{wp}$, and $P_i = 0.3bar$

Figure (10) Predicted pressure-time history at three positions along the pipe at $t_c = 40t_{wp}$, and $P_i = 0.3bar$

Figure (11-a)

Figure (11-b)

Figure (11-c)

Figure (11) Predicted stress-time history at three positions along the pipe at $t_c = t_{wp}$

Figure (12-a)

Figure (12-b)

Figure (12-c)

Figure (12) Predicted stress-time history at three positions along the pipe at $t_c = 20t_{wp}$
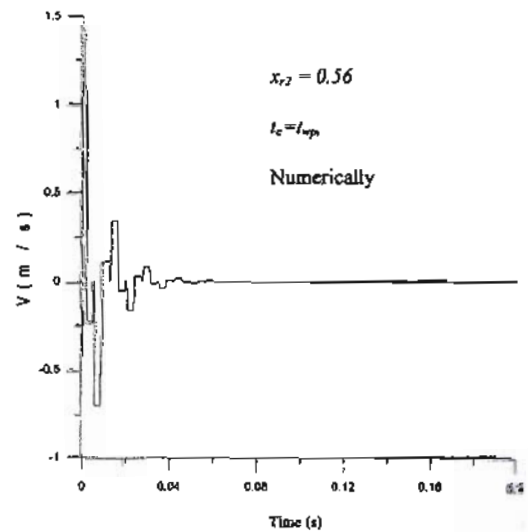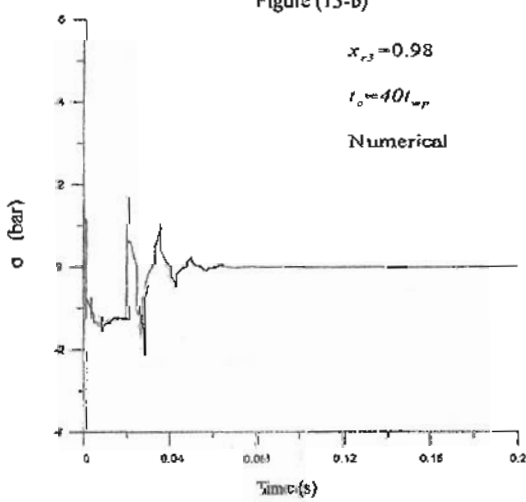
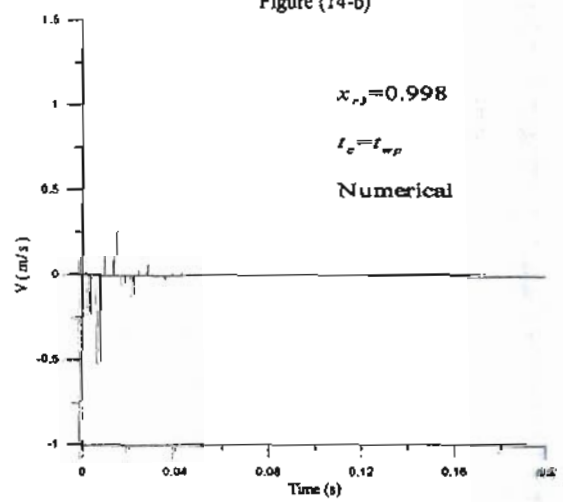Figure (13-a)

Figure (14-a)

Figure (13-b)

Figure (14-b)

Figure (13-c)

Figure (14-c)

Figure (13) Predicted stress-time history at three positions along the pipe at $t_c = 40t_{wp}$

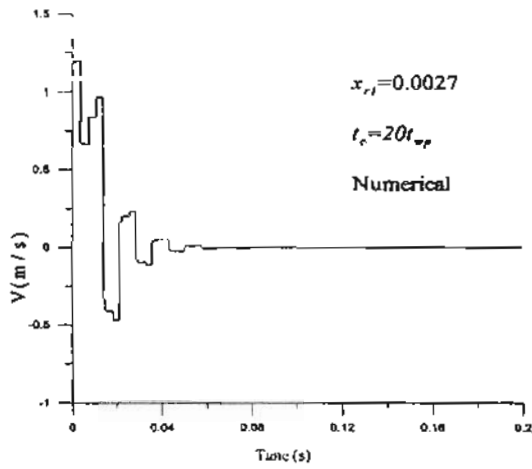Figure (14) Predicted fluid velocity-time history at three positions along the pipe at $t_c = t_{wp}$
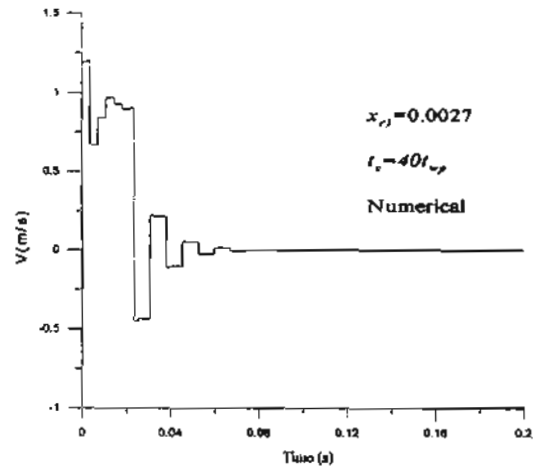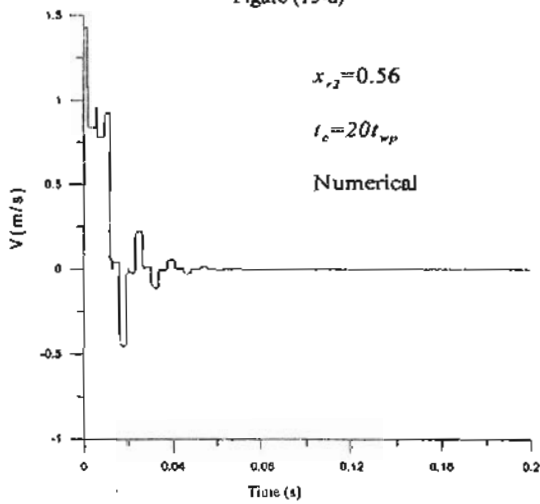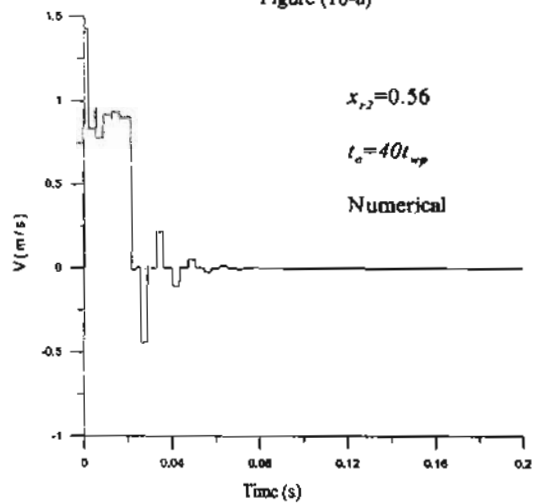
Figure (15-a)

Figure (15-b)

Figure (15-c)

Figure (15) Predicted fluid velocity-time history at three positions along the pipe at $t_c=20t_{wp}$

Figure (16-a)

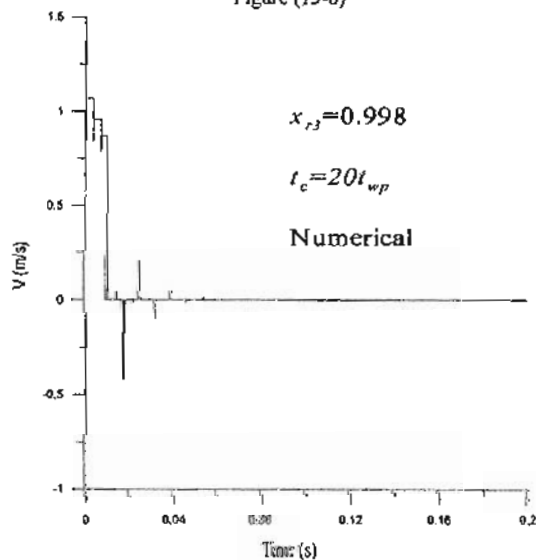Figure (16-b)

Figure (16-c)

Figure (16) Predicted fluid velocity-time history at three positions along the pipe at $t_c=40t_{wp}$

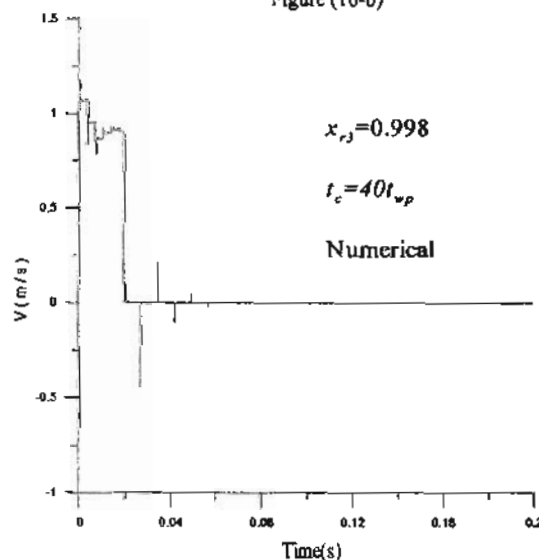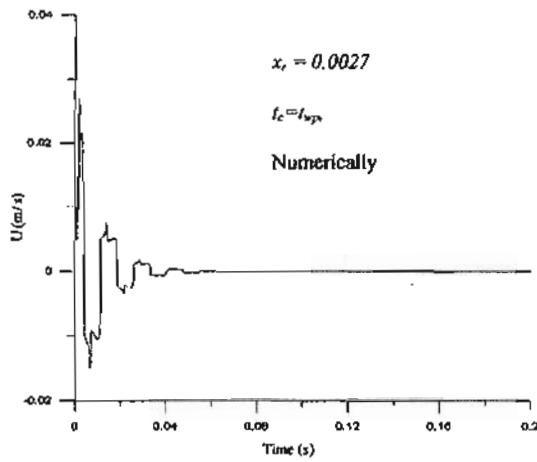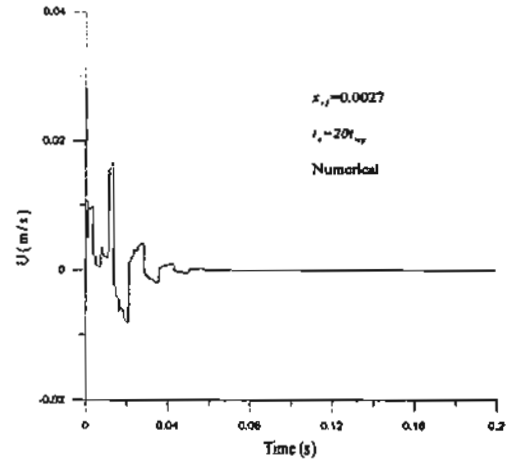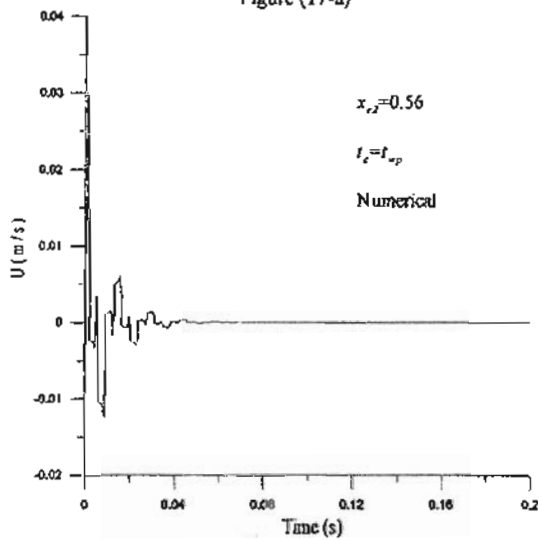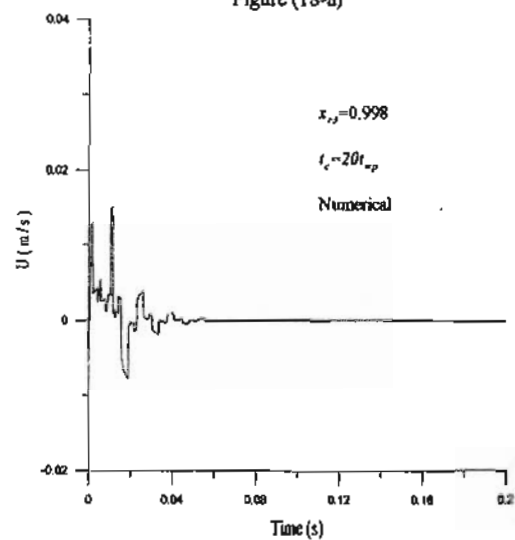Figure (17-a)

Figure (18-a)

Figure (17-b)

Figure (18-b)

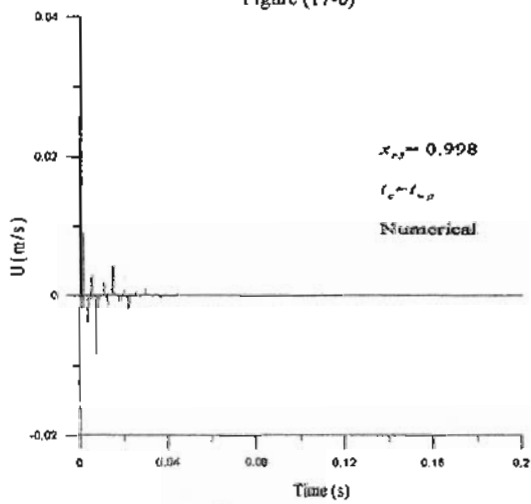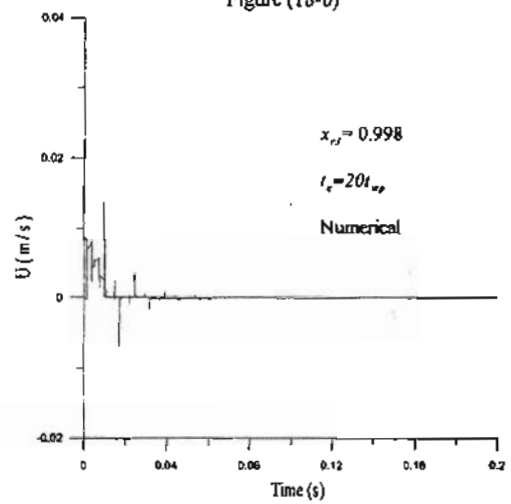
Figure (17-c)

Figure (18-c)

Figure (17) Predicted structure velocity-time history at three positions along the pipe at $t_c = t_{wp}$

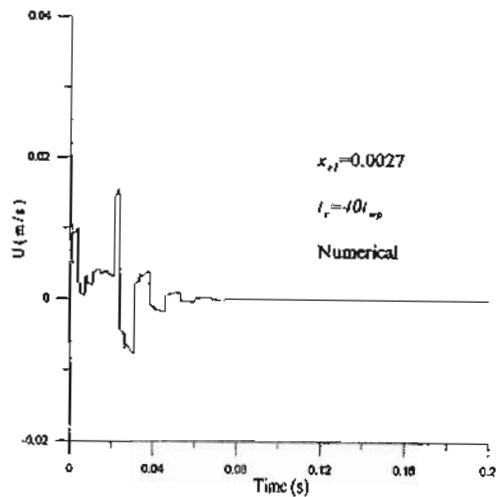Figure (18) Predicted structure velocity-time history at three positions along the pipe at $t_c = 20t_{wp}$
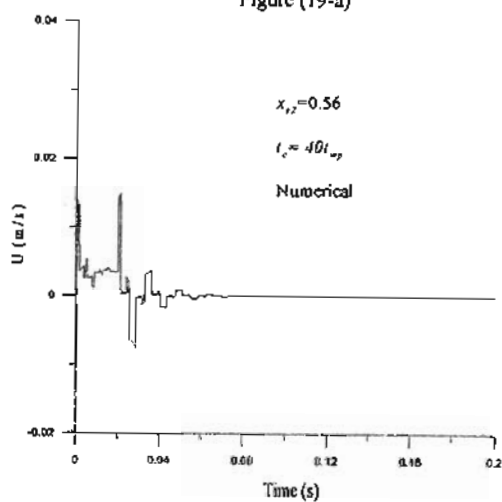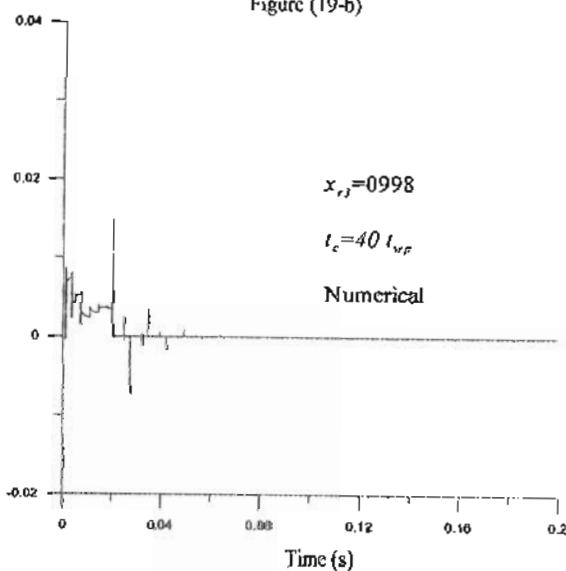
Figure (19-a)

Figure (19-b)

Figure (19-c)

Figure (19) Predicted structure velocity-time history at three positions

along the pipe at $t_c = 40 t_{wp}$

Nomenclature

A	Cross-sectional area of pipe
A_G	Valve opening area
a	Wave speed of sound
B	Pipeline characteristics impedance
	$B = a / gA$
b	Ratio of pipe density to fluid density
C_d	Orifice discharge coefficient
C_x	Viscous damping coefficient
	$C_x = 2m\omega\xi = 2\xi A_p\sqrt{E\rho_p}$
D	Inside pipe diameter
d	Ratio of pipe radius to wall thickness
E	Young's modulus of elasticity
e	Thickness of pipe wall
f	Friction factor
g	Acceleration due to gravity
H	Instantaneous piezometric head
H_0	Initial head
K	Bulk modulus of elasticity
K^*	Modified bulk modulus of elasticity
	$K^* = K \left/ \left[1 + \dfrac{DK}{eE}\left(1 - \nu^2 \right) \right] \right.$
L	Pipe length
m	Mass of system
N	Number of nodes
P	Fluid pressure at pipe centerline
P_i	Initial Pressure
P_{sh}	Shutoff pressure
Q_0	Steady-state flow rate
R	Resistance coefficient
	$R = f\Delta x/(2gDA^2)$
R_e	Reynolds number $R_e = \rho VL/\mu$
r_i	inner radius of Pipe
r_0	outer radius of Pipe
t	Time
U	Displacement of pipe in axial direction
$\dot{U}$	Structure velocity
V	Average velocity of fluid
V	Volt
W	Weighting function used in friction term
x	Distance
x_{rl}	Dimensionless distance from the pump (x/ L)

Greek Symbols

α	Angle of inclinations of the pipeline with the horizontal	σ	Pipe axial stress
β	Time used in convolution integral	ξ	Damping ratio($\xi = C_x / 2m\omega$)
ρ	Density	ω	Circular frequency $\quad \omega^2 = \frac{K}{m} = \frac{AE}{mL}$
ν	Poisson ratio for pipe material	λ	Modified wave speed
μ	Absolute viscosity	Δt	Time step in space-time grid

τ_θ Fluid   shear   stress   at   wall

$$\tau_o = \frac{8\rho_f \mu_f}{D}\bar{V}(t) + \frac{4\rho_f \mu_f}{D}\int_0^t \frac{\partial \bar{V}}{\partial t}(\beta)w(t-\beta)du$$

Δx Distance associated with Δt in space-time grid

Subscripts

f	Fluid	p	Pipe
o	Steady state	r, θ, x	Principle cylindrical coordinate directions

Abbreviations

MOC   Method Of Characteristics

WHPUMP2   Water Hammer, with Pump at Upstream end, and using two equations model

WHPUMP4   Water Hammer, with Pump at Upstream end, and using four equations model

REFERENCES

1- **Bergant, A., and Tijsseling, A.,** "Parameters affecting water hammer wave attenuation shape and timing", Proceedings of the 10th International Meeting of the Work Group on the Behavior of Hydraulic Machinery under Steady Oscillatory Conditions, Stuttgart, Germany, Trondheim, Norway, June 26, 2001; 11 pages.

2- **Budny, D. D., Wiggert, D. C., and Hatfield, F. J.,** "The influence of structure damping on internal pressure during a transient pipe flow", ASME Journal of Fluids Engineering, Sep. 1991; Vol. 113, PP.424-429.

3- **Elansary, A. S., and Contractor, D.N.,** "Valve closure: method for controlling transients", ASME Journal of Pressure Vessel Technology, Nov. 1994; Vol. 116, PP. 437-442.

4- **Fan, D., and Tijsseling, A.,** "Fluid structure interaction with cavitation in transient pipe flow", ASME Journal of Fluids Engineering, June 1992; Vol. 114, PP. 268-274.

5- **Hawam,** "Water hammer in pipeline", M. Sc. Thesis, Faculty of Engineering, Mansoura University El-Mansoura, Egypt, 2000.

6- **Kerh, T., Lee, J. J., and Wellford, L. C.,** "Transient fluid structure interaction in a control valve", ASME Journal of Fluids Engineering, June 1997; Vol. 119, PP. 354-359.

7- Ismaier. A., Schlücker. E., "Fluid dynamic interaction between water hammer and centrifugal pumps", Nuclear Engineering and Design 239, 2009. PP. 3151-3154. (E-mail address: is@ipat.uni-erlangen).

8- **Kratz, J., Munch, W., and Ungar, K.,** "The influence of fluid-structure interaction on pipe system loads", 17th International Conference on Structure Mechanics in Reactor Technology (SMIRT) Prague, Czech Republic, Aug. 17-22, 2003.

9- **Djebedjian, M. A., Mohamed, M. S., Mondy, A., and B. Rayan,** "Cost optimization of water distribution systems subjected to water hammer", Thirteenth International Water Technology Conference, Hurghada, Egypt. 2009. PP. 491-513.

10- **Redaelli, L.,** "Numerical approximation of fluid structure interaction problems", M.

Sc. Thesis, Faculty of Engineering, Politecnico di Milano University, Milano- (I), 2002.

11- Nieves, V. R., "Static and dynamic analysis of piping system", M. Sc. Thesis, Faculty of Engineering, University of Puerto Rico, Mayaguez Campus, Dec. 2004.

12- Sato, S., Taketomi, T., and Suzuki, K., "Improving Zielke method of simulating frequency-dependent friction in laminar liquid pipe flow", ASME Journal of Fluids Engineering, Dec. 1991; Vol. 113, PP. 569-573.

13- Stuckenbruck, S., Wiggert, D. C., and Otwell, R. S., "The influence of pipe motion on acoustic wave propagation", ASME Journal of Fluids Engineering, Dec. 1985; Vol. 107, PP. 518-522.

14- Thorley, A.R.D., "Pressure transient in hydraulic pipelines", Journal of Basic Engineering, September 1969; PP. 453-461.

15- Tijsseling, A.S., "Exact solution of linear hyperbolic four-equation system in axial liquid-pipe vibration", Journal of Fluids and Structures, July 2003; Vol. 18, PP. 179-196.

16- Tijsseling, A.S., "Water hammer with fluid-structure interaction in thick-walled pipes", Computers and Structures 85, 2007, PP. 844-851.
E-mail address: (a.s.tijsseling@tue.nl)

17- Tijsseling, A.S., " Exact Computation of The Axial Vibration of Two Coupled Liquid Filled Pipes", Centre for Analysis, Scientific computing and Applications Department of Mathematics and Computer Science Eindhoven University of Technology, May 2009, E-mail address: (a.s.tijsseling@tue.nl)

18- Walker, J .S., and Phillips, J. W., "Pulse propagation in fluid filled tubes", ASME Journal of Applied Mechanics, Mar. 1977; Vol. 44, PP. 31-35.

19- Wiggert, D. C., Otwell, R. S., and Hatfield, F. J., "The effect of elbow restraint on pressure transients", ASME Journal of Fluids Engineering, Sep. 1985; Vol. 107, PP. 402-406.

20- Wylie, E. B., and Streeter, V. L., "Fluid transients", McGraw-Hill, International Book Company, 1993.

21- Morris, J., and Dutton, C., "The performance of two butterfly valves mounted in series", ASME Journal of Fluids Engineering, 1991; Vol. 113, PP. 419-423.